Analysis and Control of Modified DC-DC Cuk Converter

Sofyan M. Ilman
School of Electrical Engineering and Informatics
Bandung Institute of Technology
Bandung, Indonesia
sofyanmuhammadilman@students.itb.ac.id

Andriazis Dahono
School of Electrical Engineering and Informatics
Bandung Institute of Technology
Bandung, Indonesia
andriazis@students.itb.ac.id

Muhammad Aji K. Prihambodo
School of Electrical Engineering and Informatics
Bandung Institute of Technology
Bandung, Indonesia
ajikunp@students.itb.ac.id

Bintang Antares Y. Putra
School of Electrical Engineering and Informatics
Bandung Institute of Technology
Bandung, Indonesia
bintang.antares@students.itb.ac.id

Arwindra Rizqiawan
School of Electrical Engineering and Informatics
Bandung Institute of Technology
Bandung, Indonesia
windra@stei.itb.ac.id

Pekik A. Dahono
School of Electrical Engineering and Informatics
Bandung Institute of Technology
Bandung, Indonesia
padahono@stei.itb.ac.id

***Abstract*—This paper proposes a control method for the modified dc-dc Cuk converter. The proposed modified dc-dc Cuk converter has an advantage compared to the conventional dc-dc Cuk converter. The output voltage polarity of this proposed converter is not reversed as in the conventional dc-dc Cuk converter, while the input and output currents are continuous similar to the conventional dc-dc Cuk converter. To control the proposed converter, a simple double loop controller is used. The outer loop controller is controlling the output voltage and the inner loop controller is controlling the inductor current. The inner loop and the outer loop are designed as propotional-integral (PI) control. The analytical approach for designing the control scheme is conducted by linearizing the small-signal model of the proposed converter to form the inductor current and output voltage transfer functions. These transfer functions will be analyzed by using phase and gain margin aproach to obtain the control parameters (Kp, Ki, and Ti). Simulated and experimental results are included to show the validity of the proposed concept.**

Keywords— DC-DC Converter, Control, Cuk, Boost.

I. INTRODUCTION

A dc-dc converter is commonly used in battery charger/discharger such as the one in dc microgrid and automotive systems. In such applications, high voltage gain and low input and output ripples are desirable. At present, the most common dc-dc converters used for these applications are dc-dc boost converter. Though the input current ripple is low, the output current ripple of this converter is high. Another converter that can be used is the conventional dc-dc Cuk converter. This converter is named after its inventor, Slobodan Cuk, in 1977. This converter is obtained by using the duality principle on the circuit of buck-boost converter [1] and then the ripple in continuous input and output current of this converter is low [2]. In its application, dc-dc Cuk converter is combined with a Sepic converter for the microgrid and smart grid [3][4].

A lot of literature have discussed the control of the dc-dc converter to solve the problem in managing the converter system performance that can work independently from various disturbances, whether classical control theory or based modern control. Modern control such as fuzzy logic controller, loop shaping method, nonlinear method and sliding mode with time scale are successful in controlling the Cuk converter [5]-[8]. The classical control theory used to control the Cuk converter, such as PI, sliding mode with Routh–Hurwitz, root locus method cascaded PI- CSMC (continuous sliding mode controller), and robust controller also proved to be successful in controlling the system [9]-[11].

This paper presents a newly designed partial rated Cuk converter. The difference in the proposed converter is that the output voltage polarity is not reversed. A simple double loop PI controller, which consists of outer output voltage loop control and the inner current loop control, is used to control this converter. The analytical approach is done by linearizing the small-signal model of the converter to produce the inductor current and output voltage transfer function. From the Bode plot and phase margin analysis, we will obtain the controller parameter values. An experiment will be done to prove the control system performance.

II. MODIFIED CUK CONVERTER

Basic principles of the modified dc-dc Cuk converter are discussed here. The dc-dc converter is the modification result of Cuk dc-dc [12]. Fig.1 (a) shows the basic of the Cuk dc-dc converter is the dual of buck-boost dc-dc converter. Under continuous conduction mode, it can be shown that the output voltage ratio is:

$$\frac{\bar{v}_o}{E_d} = \frac{\alpha}{1-\alpha} \tag{1}$$

where

$$\alpha = \frac{T_{ON}}{T_s} \tag{2}$$

is the duty cycle factor of transistor Q and T_s is the switching period. The converter has the ability to produce an output

978-1-7281-2669-2/19/$31.00 ©2019 IEEE

voltage that is lower or higher of the dc input voltage side. The converter has continuous input and output currents with the associated low ripple content. However, the polarity of the dc output voltage side is reversed. Fig.1(b) is the redrawn scheme of the converter. As it is shown in Fig. 1(b), there is a third terminal with output voltage ratio as follow:

$$\frac{\bar{v}_o'}{E_d} = \frac{1}{1-\alpha} \tag{3}$$

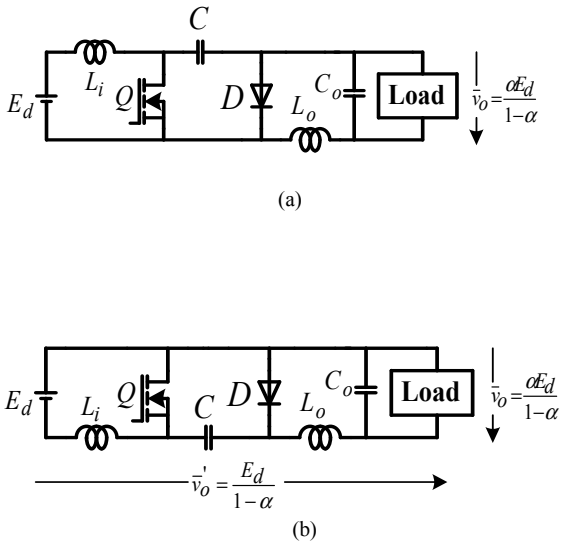

The output voltage has an output voltage that is higher than the conventional output terminal. But, polarity the voltage of this third terminal is not reversed.

If the load is connected to the third terminal then the modified dc-dc Cuk converter can be obtained as shown in Fig. 1(c). The output voltage has an output voltage that is higher than the conventional dc-dc Cuk converter. The output voltage polarity is not reversed. The input and output currents are continuous similar to dc-dc Cuk converter.

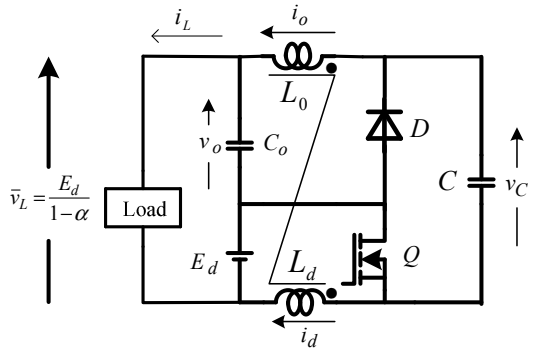

Fig. 1. Modification of Cuk converter.

III. CLOSED LOOP DESIGN

A. Closed Loop Design

The circuit configuration in Fig.2 can be modeled into the small-signal model of the converter by deriving the circuit KCL and KVL equation to produce state-space averaging form. Then, linearization will be done to the state-space averaging form to produce the small-signal model in the matrix equation. The small-signal model of the converter is given in equation (4) and (5).

The transfer functions such as control-to-output transfer function, control-to-input current transfer function, and current-to-output transfer function are obtained from equation (4) and (5) are stated in equation (6) and (7), where $\widehat{I_d}$ is the inductor L_d current, $\hat{d}$ is the duty cycle, $\widehat{I_o}$ is inductor L_o current, and $\widehat{V_o}$ is the output voltage.

The bandwidths of the current and voltage loop are separated far apart as the voltage loop is slower and the current loop is faster. The block diagram of the PI controller is represented in Fig.2 the inner current loop control and outer voltage loop control transfer function stated in equation (7) will regulate the output voltage of the converter.

B. Inner Current Loop Control (Id)

The design of inner current loop control for inductor L_d is represented in Fig.4 with load current disturbance *(IL),* which involves defining the current loop quantitatively and should meet the design criteria of phase margin (PM) and bandwidth or crossover frequency. The inner current loop has faster dynamics than the outer voltage loop. Therefore, the inductor currents can change more quickly than the output voltage because of the existence of time scale separation between both loops and state variables. This can be exploited to simplify the controller design. Then, we input the converter specification value from Table 1 to obtain the transfer function value. The Bode plot of the transfer function in equation (5) is shown in Fig. 5.

$$T_{OL1}(s) = T_{c1}(s).T_{p1}(s).H_1(s).T_m(s) \tag{8}$$

The transfer function of PI-controller ($T_{c1(s)}$) is defined by:

$$T_{c1}(s) = K_p + \frac{K_i}{s} \tag{9}$$

$H_1(s)$ equation (8) is an expression of current sensor Id. By assuming 100% accuracy at the current sensor in L_d, then the feedback gain will be:

$$H_1(s) = 1 \tag{10}$$

The transfer function of the modulator ($T_m(s)$) is defined by:

$$T_m(s) = \frac{1}{V_{m,p-p}} \tag{11}$$

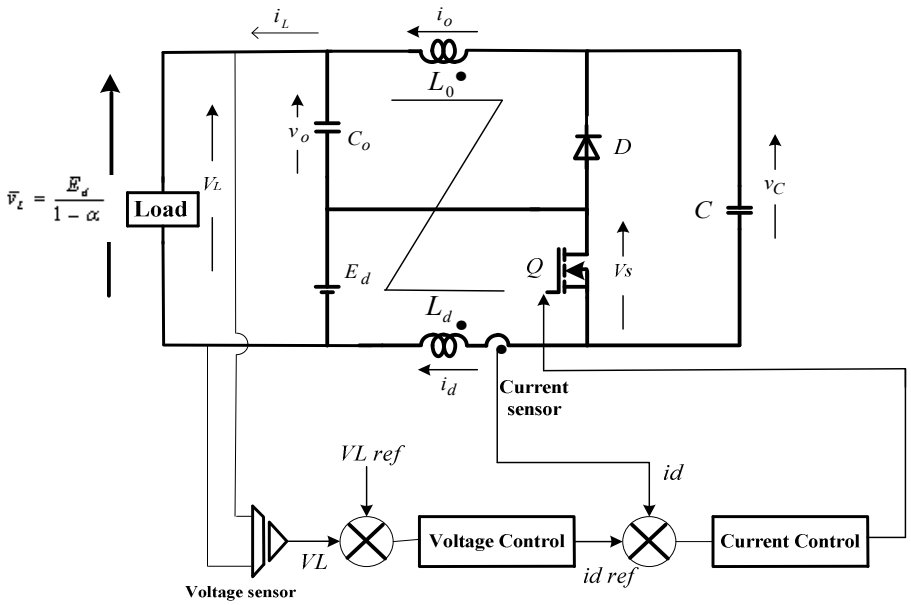

Fig. 2. Modified dc-dc Cuk converter with double loop control.

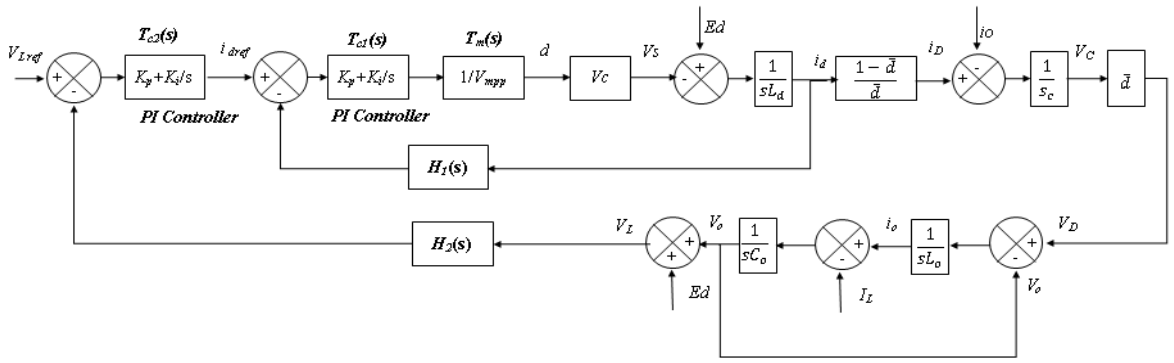

Fig. 3. Block diagram of double-loop control.

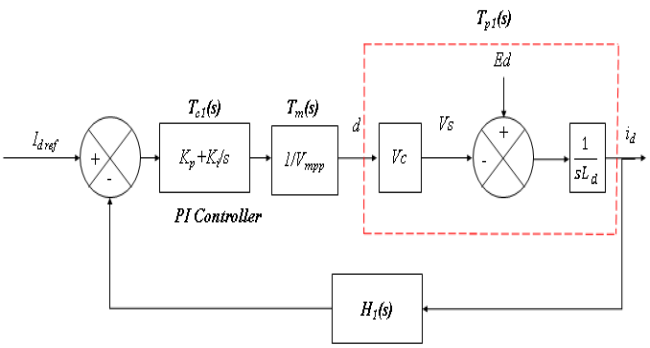

Fig. 4. Block diagram of inner current *(Id)* loop control.

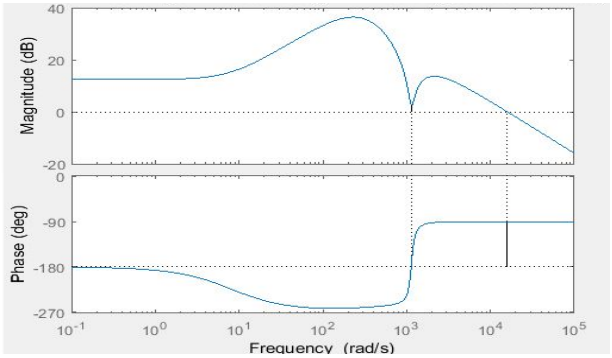

Fig. 5. Bode plot of current loop

$$\begin{bmatrix} sLd & 0 & -(1-D) & 0 \\ 0 & sLo & -D & 1 \\ -(1-D) & D & sC & 0 \\ 0 & -1 & 0 & -sCo \end{bmatrix} \cdot \begin{bmatrix} \widetilde{I_d} \\ \widetilde{I_o} \\ \widetilde{Vc} \\ \widetilde{VL} \end{bmatrix} = \begin{bmatrix} 1 \\ 1 \\ 0 \\ -sCo \end{bmatrix} \widetilde{Ed} + \begin{bmatrix} Vc \\ Vc \\ I_o - I_d \\ 0 \end{bmatrix} \tilde{\mathrm{d}} + \begin{bmatrix} 0 \\ 0 \\ 0 \\ 1 \end{bmatrix} \tilde{\mathrm{I}}\mathrm{L} \quad (4)$$

$$\begin{bmatrix} \widetilde{I_d} \\ \widetilde{I_o} \\ \widetilde{Vc} \\ \widetilde{VL} \end{bmatrix} = \begin{bmatrix} sLd & 0 & -(1-D) & 0 \\ 0 & sLo & -D & 1 \\ -(1-D) & D & sC & 0 \\ 0 & -1 & 0 & -sCo \end{bmatrix}^{-1} \begin{bmatrix} Vc \\ Vc \\ I_o - I_d \\ 0 \end{bmatrix} \tilde{d} + \begin{bmatrix} sLd & 0 & -(1-D) & 0 \\ 0 & sLo & -D & 1 \\ -(1-D) & D & sC & 0 \\ 0 & -1 & 0 & -sCo \end{bmatrix}^{-1} \cdot$$

.

$$\begin{bmatrix} 1 \\ 1 \\ 0 \\ -sCo \end{bmatrix} \widetilde{Ed} + \begin{bmatrix} sLd & 0 & -(1-D) & 0 \\ 0 & sLo & -D & 1 \\ -(1-D) & D & sC & 0 \\ 0 & -1 & 0 & -sCo \end{bmatrix}^{-1} \begin{bmatrix} 0 \\ 0 \\ 0 \\ 1 \end{bmatrix} \tilde{\mathrm{I}}\mathrm{L} \quad (5)$$

$$\frac{\widehat{I_d}}{\hat{d}} = \frac{(L_d C C_o V_C)s^3 + (C L_d V_C + (I_d - I_o)(L_d C_o D)s^2 +}{(L_d L_o C C_o)s^4 + (C L_d L_o)s^3 + (2L_o C_o D + D^2 C_o(L_d - L_o) - C L_d - L_o C_o)s^2 +}$$

$$\frac{(-C_o V_C + 2DV_C C_o - D^2 C_o V_C - (I_d - I_o)DL_d - V_C(D-1)C_o D)s + 2DV_C - D^2 V_C - V_C - V_C(D-1)D}{(2DL_o - L_o + D^2 L_d - D^2 L_o)s + D^2 - 2D} \quad (6)$$

$$\frac{\widehat{V_L}}{\widehat{I_d}} = \frac{(L_d C C_o V_C)s^3 + (C L_d V_C + (I_d - I_o)(D-1)C_o L_d)s^2 +}{(L_d C C_o V_C)s^3 + (C L_d V_C + (I_d - I_o)(L_d C_o D)s^2 +}$$

$$\frac{((D^2 C_o - C)V_C - (DC_o - D^2 C_o)V_C + (I_d - I_o)(D-1)L_o)s + D^2 V_C - V_C(D - D^2) + (I_d - I_o)(D-1)}{(-C_o V_C + 2DV_C C_o - D^2 C_o V_C - (I_d - I_o)DL_d - V_C(D-1)C_o D)s + 2DC_C - D^2 V_C - 2V_C(D-1)D} \quad (7)$$

Therefore, the transfer function will be:

$$T_{OL1}(s) = \left(K_p + \frac{K_i}{s}\right).T_{p1}(s).H_1(s).T_m(s) \quad (12)$$

The relation between the inductor current (I_{Ld}) and reference current (I_{ref}) when all disturbances are insignificant or very small, can be represented by equation (13).

$$\frac{I_d(s)}{I_{dref}(s)} = \frac{T_{c1}(s).T_{p1}(s).T_m(s)}{1 + T_{c1}(s).T_{p1}(s).H_1(s).T_m(s)} \quad (13)$$

With phase margin (PM)= 90° is obtained at ($\omega c = 1{,}59.10^4$ rad/sec). These values will be used in PI-controller calculation to produce K_p, K_i , and Ti value. By substituting the final equations from gain condition and phase angle condition, we obtain K_p=0,046, K_i = 3,6, and Ti=$1.4x\ 10^{-3}$.

C. Outer Output Voltage Loop Control(Vo)

The design of outer output voltage loop control for V_o is represented in Fig.6 with input voltage disturbance *(Ed)*. It involves defining the output voltage loop quantitatively, which should meet the design criteria of phase margin (PM) and bandwidth or crossover frequency. From fig.4 we obtain the equation of output voltage transfer function. The transfer function output voltage will be compared with the current transfer function. The output voltage transfer function ($T_{p2}(s)$) is represented by equation (7). Bode plot of the transfer function in equation (7) is represented in Fig.7. The voltage reference selected will be 40 V,

$$T_{OL2}(s) = T_{c2}(s).T_{p2}(s).H_2(s) \quad (14)$$

TABLE I. CONVERTER SPECIFICATION

Component	Value	Unit
Ld	2.5	mH
Lo	2.5	mH
C	2200	µF
Co	1000	µF
V_o	40	V
V_{in}	36	V
R	22	Ω
f	10	kHz

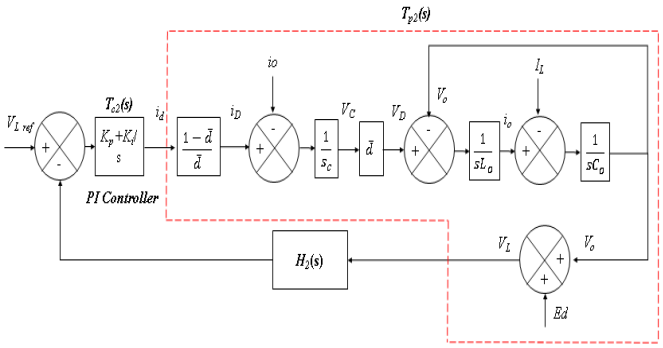

Fig. 6. Block diagram of outer output voltage (Vo) loop control..

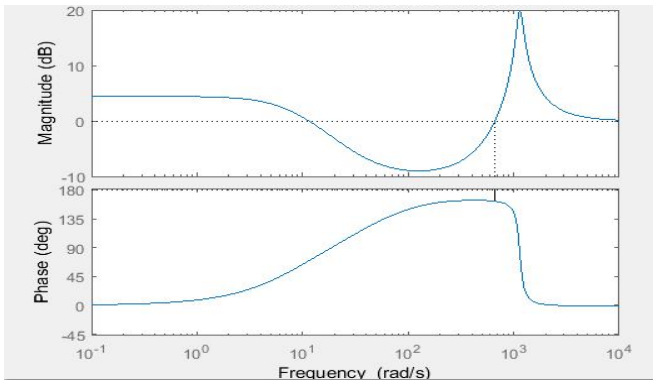

Fig. 7. Bode plot of output voltage loop.

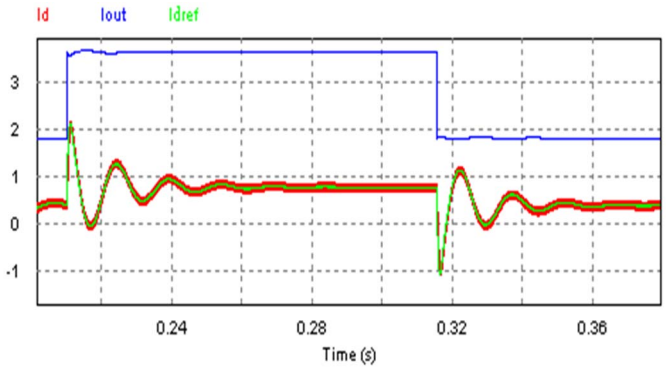

Fig. 8. Simulation result of the current control *(Id)*.

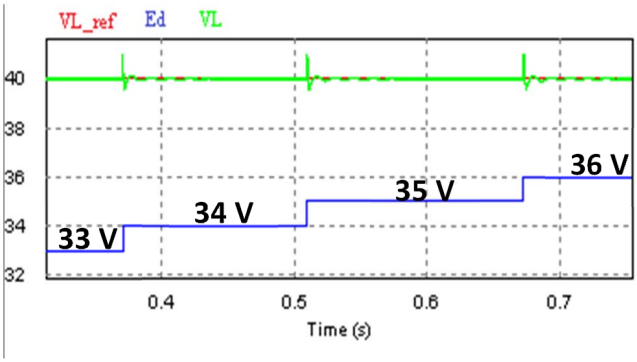

Fig. 9. Simulation result of output voltage with input voltage 33 V, 34 V, 35 V, and 36 V.

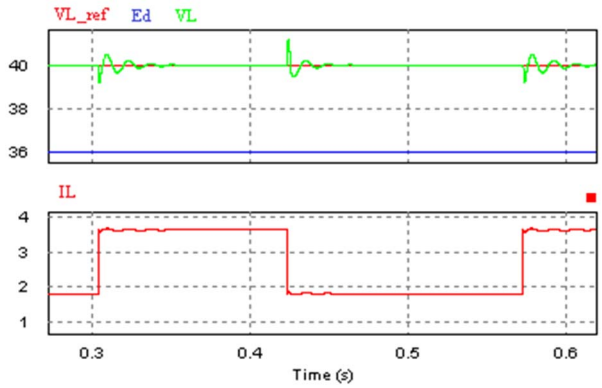

Fig. 10. Simulation result if output current during load changes with input voltage 36 V.

The transfer function of PI-controller ($T_{c2}(s)$) is defined by:

$$T_{c2}(s) = K_p + \frac{K_i}{s} \quad (15)$$

Therefore, the transfer function will be:

$$T_{OL2}(s) = \left(K_p + \frac{K_i}{s}\right).T_{p2}(s).H_2(s) \quad (16)$$

The crossover frequency (ω_c) of 666 rad/sec is obtained from the bode plot. In the phase angle condition, the phase angle of the loop is PM-180^0. From bode plot, we obtain PM = 120^0 so that the $T_{OL2}(s)$ = 120^0-180^0 = -50^0. By substituting the final equations from gain condition and phase angle condition, we obtain K_p= 1,87, K_i= 545,81, and Ti=3,42x10^{-3}. Fig.8 shows that the simulation of the current control (Id) works well, while Fig.9 and 10 shows that the simulation of the output voltage control is also works well in different cases.

IV. EXPERIMENTAL RESULTS

An experiment is conducted to validate the PI controller performance. The modified dc-dc Cuk components used in the experiment is corresponded with the value showed in Table 1.

A. Case-1 Input Voltage Fluctuation

The experiment waveform in Fig.11 shows the waveform of output, input, and the reference voltage. The output voltage is aimed to stay at 40 V, while the input voltage is fluctuating between 33-36 V. It can be seen that the output voltage is steady-state on the reference, although the input voltage is fluctuating.

B. Case-2 Condition During Load Changes

Fig.12 shows the waveform of the output voltage, input voltage, output voltage reference, and output current during a load change. Although the load is changing, the controller can keep the output voltage steady-state on voltage reference.

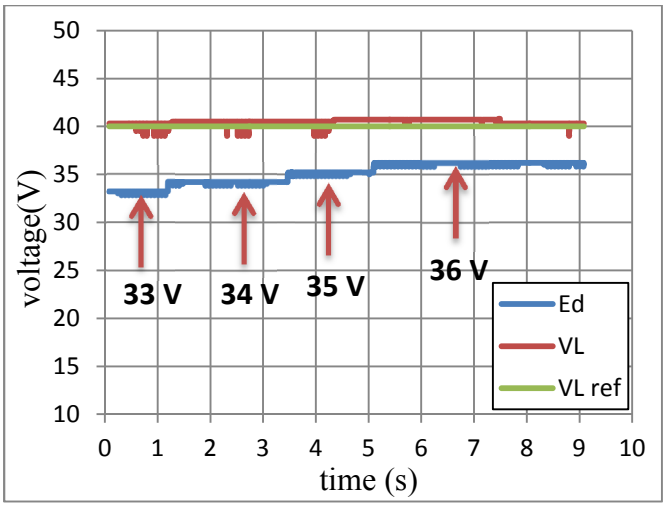

Fig. 11. Experiment result of output voltage with input voltage 33 V, 34 V, 35 V, and 36 V.

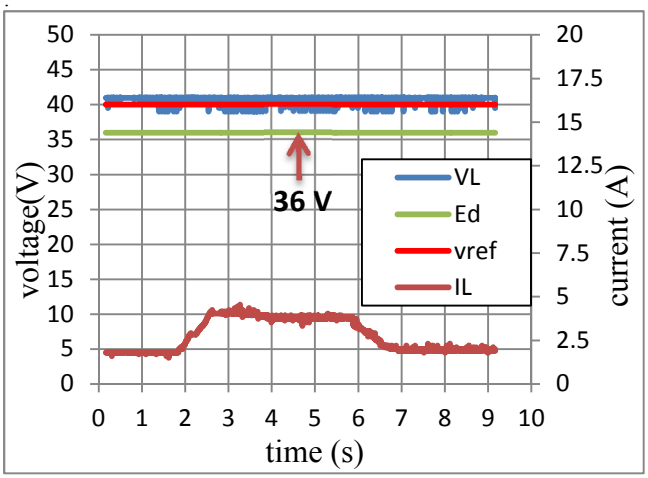

Fig. 12. Experiment result of output voltage during load changes with input voltage 36 V.

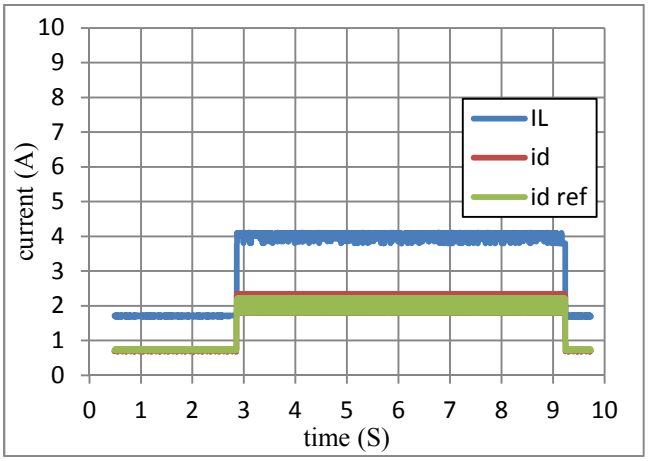

Fig. 13. Experiment result of current control (Id).

V. CONCLUSION

In this paper, the authors has designed a control method for the modified dc-dc Cuk converter using a simple double loop PI controller for controlling the output voltage and current. The design is done by doing analytical calculations and software simulation. The experimental, which meant to validate the design proposed, has shown satisfying results. The double loop PI can control the current and output voltage at a steady state in all cases that have been described.

ACKNOWLEDGMENT

The authors wish to thank Ministry of Research, Technology, and Higher Education of Indonesia, LPDP, PT. LEN Industry, and KOMIPO for providing research funds of this work.

REFERENCES

[1] Ned Mohan, Power Electronics, University of Minnesota, Thrid Edition, 2003.

[2] Muhammad H.Rashid, Power Electronics Handbook, University of Florida, 2001.

[3] Devika P V, Rosemin Parackal, "SEPIC-CUK Converter For PV Application Using Maximum Power Point Tracking Method," International Conference on Control, Power, Communication and Computing Technologies (ICCPCCT), pp.266, March 2018..

[4] Arun Shastry P S, Suresh K V, Vinayaka K U "Hybrid Wind-Solar Systems using Cuk-Sepic Fused Converter with Quasi-Z-Source Inverter," International Conference on Communication and Signal Processing, Oct 2015.

[5] Saptarshi Rakshit, Jayabrata Maity, "Fuzzy Logic Controlled Ćuk Converter," Power, Communication and Information Technology Conference (PCITC), pp.0771, April 2018.

[6] Zeeshan Rayeen, Sourav Bose, Prakash Dwivedi, "Study of Closed loop Cuk converter controlled by Loop Shaping Method," International Conference on Industrial and Information Systems (ICIIS), pp.442-446, 2018.

[7] Kurt Schlacher, Andreas Kugi, "Modern Control of a Ćuk Converter Using Nonlinear Methods," IEEE International Conference on Control and Applications, pp.503, August 1994.

[8] Snehal B. Gaikwad, Shilpa D. Joshi, "Design of Cuk Converter based Three Phase Inverter by Fuzzy Controller," International Conference on Computing, Communication, Control and Automation (ICCUBEA), August 2017.

[9] Efim A.Aksenov, Valery D.Yurkevich, "Sliding Mode and Time-Scales in Control System Design for a Cuk Converter," International Conference On Micro/Nanotechnologies And Electron Devices EDM, pp.401-402, 2016.

[10] Zengshi Chen, "PI and Sliding Mode Control of a Cuk Converter," IEEE Transactions On Power Electronics, Vol. 27, No. 8, pp.3695-3696, August 2012.

[11] Fiaz Ahmad, Akhtar Rasool, Emre Ozsoy, Asif Sabanoviç, M. Elitas, "Design of a Robust Cascaded Controller for Cuk Converter," pp.80-81, 2016.

[12] S. Cuk and R. D. Middlebrook, A New Optimum Topology Switching DC-DC Converter, IEEE Power Electr. Spec. Conf. Rec., 1977, pp. 160-179.